Am J Transl Res 2026;18(3):1863-1878
www.ajtr.org /ISSN:1943-8141/AJTR0171256

Original Article

Aquaporin-1 upregulation is associated with scleral remodeling during myopia development in mice

Weihua Zhang[1,2], Yan Cheng[3,4], Jiayin Wu[5], Xiaodong Jia[3,4], Hongxia Gao[2], Jinqiang Yan[6], Weijing Li[2], Cuiying Zhang[2], Xue Wang[2], Jianlu Gao[1,2]

[1]Department of Ophthalmology, Liaocheng People's Hospital, Shandong University, Jinan 250012, Shandong, China; [2]Department of Ophthalmology, Liaocheng People's Hospital, Liaocheng 252000, Shandong, China; [3]Joint Laboratory for Translational Medicine Research, Liaocheng People's Hospital, Liaocheng 252000, Shandong, China; [4]Key Laboratory of Ophthalmology, Liaocheng People's Hospital, Liaocheng 252000, Shandong, China; [5]Department of Ophthalmology, Qilu Hospital of Shandong University, Jinan 250014, Shandong, China; [6]Department of Pathology, Liaocheng People's Hospital, Liaocheng 252000, Shandong, China

Received January 5, 2026; Accepted February 25, 2026; Epub March 15, 2026; Published March 30, 2026

Abstract: Objective: To determine the functional importance of aquaporin-1 (Aqp1) in scleral remodeling during myopia development using *in vivo* and *in vitro* models. Methods: Forty-two C57BL/6J mice were randomly assigned into experimental (n=28) and normal control (NC) groups (n=14). In the experimental group, the right eyes underwent form deprivation (deprived eye, DE), whereas the left eyes served as self-controls (fellow eye, FE). Mice in the normal control (NC) group received no treatment in either eye. Refraction was measured before and after myopia induction, and axial length was measured at the end of the experiment. The expression levels of Aqp1, hypoxia-inducible factor-1 alpha (Hif-1α), matrix metallopeptidase 9 (Mmp9), and collagen type I alpha1 (Col1α1) in sclera were determined by immunofluorescence staining, qRT-PCR, and/or western blotting. Scleral morphology was evaluated using hematoxylin and eosin staining. Results: After two weeks of form-deprivation, DE eyes exhibited a significant myopic shift (1.66±0.09 D) compared with FE eyes (4.92±0.06 D) and NC eyes (left: 4.78±0.11 D; right: 4.91±0.10 D). Scleral thinning was found in DE eyes. Expression levels of Aqp1, HIF-1α, and Mmp9 were significantly upregulated, whereas Col1α1 expression level was significantly downregulated in DE eyes compared to FE and NC eyes. *In vitro*, hypoxic exposure significantly increased Aqp1 expression level in human scleral fibroblasts (HSFs). Aqp1 overexpression induced a concomitant upregulation of Mmp9. Conversely, treatment with 200 mM acetazolamide under hypoxic conditions inhibited the expression levels of both Aqp1 and Mmp9. Conclusions: The findings indicated that Aqp1 upregulation was associated with scleral remodeling during myopia development and Aqp1 could contribute to this process, at least in part, through regulation of Mmp9 expression level.

Keywords: Myopia, scleral remodeling, Aqp1, form-deprivation, HSFs, Mmp9

Introduction

Myopia has emerged as a major public health concern, with its prevalence increasing rapidly among adolescents and young adults, particularly in East Asia [1]. This condition can lead to severe ocular complications, including cataract, glaucoma, retinal and macular degeneration, and even blindness [2-6]. Therefore, a comprehensive understanding of the mechanisms underlying myopia onset and progression is essential for developing effective preventive and therapeutic strategies.

Fibroblasts play a notable role in maintaining scleral integrity and contribute significantly to ocular refraction and the pathogenesis of myopia [7, 8]. Structural remodeling of the sclera, characterized by collagen degradation and alterations in the extracellular matrix (ECM), has been identified as a key process mediating axial elongation in myopic eyes [9]. Consequently, both scleral tissue and fibroblast function have become central focuses in myopia research [10].

Aquaporins (AQPs) are a group of transmembrane proteins that participate in modulating water transportation and ECM [11, 12]. Aquaporin-1 (Aqp1), the first identified member of this family, has been documented to be

https://doi.org/10.62347/CLED5034

involved in collagen metabolism and tissue remodeling [13, 14]. Aqp1 has been reported to affect the biomechanical strength of sclera, reflecting its potential contribution to myopia pathogenesis [15]. Furthermore, earlier studies have identified expression level of Aqp1 in scleral fibroblasts of rats and human beings [16], while its expression level in murine sclera has not yet been documented.

According to recent investigations, Aqp1 plays important roles in ECM remodeling by regulating collagen synthesis, organization, and degradation in different tissues [17, 18]. Moreover, Aqp1 depletion resulted in significant reduction in scleral biomechanical strength [15]. Additionally, Aqp1 expression level is associated with type I collagen level, which is the principal structural protein of the sclera [19]. All these findings indicate that Aqp1 is a promising candidate for investigating the mechanisms of myopia pathogenesis. Acetazolamide is also an Aqp1 inhibitor that is a potent and sulfonamide-based drug with a wide variety of clinical uses [20].

The matrix metalloproteinases (MMPs) are zinc-dependent endopeptidases with ubiquitous tissue expression and collagenolytic activity required for ECM remodeling in tissues such as the posterior ocular sclera [21]. It has been established that there is an upregulation of the expression of the matrix metalloproteinase 9 (Mmp9) in the scleral tissue of myopic murine models [22]. Moreover, multiple studies have demonstrated that Aqp1 regulates the Mmp9 expression level [15, 23].

Hypoxia-inducible factor-1 alpha (Hif-1α) is a transcription factor that regulates tissue remodeling under hypoxic conditions [24, 25]. The Hif-1α signaling pathway has been validated to induce the development of myopia through the regulation of the interaction between genetic and environmental factors [26]. It was shown that the HIF-1α level is elevated following the induction of myopia, and the pathways associated with hypoxia may lead to scleral changes [24, 26].

The transcriptional regulation of Aqp1 by HIFs has been well-documented. Hif-1α directly binds to hypoxia response elements in the Aqp1 promoter region, leading to transcriptional activation under hypoxic conditions [27]. Given that scleral hypoxia has been identified as a key driver of myopia progression [28], we hypothesized that Aqp1 may contribute to scleral remodeling in myopic eyes in a Hif-1α-dependent manner. The present study aimed to determine the presence and changes of Aqp1 in myopic sclera using a form-deprivation myopia (FDM) model and in human scleral fibroblasts (HSFs) under hypoxic condition. The findings may provide new insight into the molecular mechanisms underlying myopia development and explore the potential translational value of Aqp1.

Materials and methods

Animals

Healthy 3-week-old male C57BL/6J mice (10-15 g) purchased from Beijing Vital River Laboratory Animal Technology Co., Ltd. (Beijing, China) were housed under controlled conditions (23±2°C, 45%-65% humidity, 12-h light-dark cycle). Mice with ophthalmic diseases were excluded from this investigation [29]. All experiments were approved by the Medical Ethics Committee and the Institutional Animal Care and Use Committee of Liaocheng People's Hospital (Approval No. 2023131) and were conducted in accordance with the Association for Research in Vision and Ophthalmology Statement for the Use of Animals in Ophthalmic and Vision Research. All mice were monitored daily for weight loss, behavioral changes, and overall health. Humane endpoints included marked weight loss (≥20% of initial body weight), severe distress, inability to access food or water, complications related to the occlude, or severe ocular lesions.

FDM model induction and measurements

FDM was induced in the right eye using a translucent occlude, as previously described [10]. In brief, mice were subjected to form-deprivation in the right eye for two weeks using a custom-made translucent monocular occluder (**Figure 1**). For refraction measurements, mice were anesthetized with a combination of Zoletil 50 (Tiletamine and Zolazepam, 25 mg/kg) (Virbac, France) and xylazine (10 mg/kg) (V86522; InvivoChem, USA) intraperitoneally. Anesthesia was administered once per refraction measurement session (baseline and 2 weeks after FDM induction). Ocular refraction was measured with a streak retinoscope (YZ24; Suzhou Liuliu Vision Technology Co., Ltd., China) and

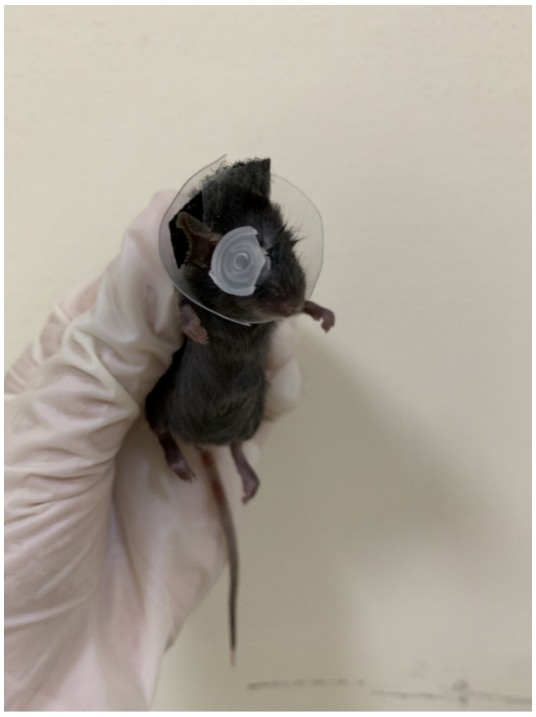

Figure 1. FDM mouse model. Representative image showing a mouse waring a monocular occluder to induce FDM.

performed using tropicamide (H20123453; Shenyang Xingqi Ophthalmic pharmaceutical Co., Ltd., China) in a dark room. During the refraction procedure, an ophthalmoscope was placed 50 cm away from eyes of mouse, and the examiner's eyes were aligned at the same level as the eyes of the mouse. The equivalent spherical diopter (calculated as the spherical diopter + 1/2 cylindrical diopter) was determined and recorded. Each eye was measured three times, and the average value was calculated. At the end of the 2-week experimental period, all mice were euthanized via CO_2 asphyxiation followed by cervical dislocation and both eyes were immediately collected for axial length measurement using a digital vernier caliper (0.01 mm precision, Delixi Electric Co., Ltd., Yueqing, China) on ice as described previously [30]. To ensure measurement accuracy, each eyeball was measured independently by a trained researcher, and each measurement was repeated three times. The final axial length was calculated as the average of all measurements.

After the FDM induction in the experimental group (n=28), mice in this group had deprived right eyes (DE) and their left eyes served as contralateral control (FE). Meanwhile, in the control group (n=14), mice with intact eyes were used as normal control (NC).

Histologic staining

For immunofluorescence staining, the eyes were embedded into optimal cutting temperature (OCT) compound on a Presto CHILL embedding system (Milestone Medical Inc., Kalamazoo, MI, USA) [31], followed by sectioning using a cryostat (Taiva/TL-820C). Then, the cryosections (4 μm) were rinsed twice with distilled water (5 min each, room temperature) and once with phosphate-buffered saline (PBS) (5 min, room temperature). Subsequently, the sections were incubated with 3% normal goat serum in PBS/0.3% Triton X-100 for 1 h at room temperature. Afterwards, sections were incubated with anti-Hif-1α (1:200, GTX127309; GeneTex, USA), anti-Aqp1 (1:200, 20333-1-AP; Proteintech Group, USA), anti-Mmp9 (1:200, 10375-2-AP; Proteintech Group, USA) and anti-Col1α1 (1:400, ab316222 Abcam, UK) antibodies overnight at 4°C, followed by incubation with goat anti-rabbit IgG (FITC) antibody (1:1,000, ab6717; Abcam, UK). Afterwards, the slides were mounted with DAPI-containing medium (S2110, Solarbio) and visualized using a fluorescence microscope (Zeiss). The fluorescence intensities were analyzed using ImageJ 1.53 software (National Institutes of Health, Bethesda, MD, USA) to reflect relative protein expression level.

For hematoxylin and eosin (H&E) staining, the tissue sections were processed using a Tissue-Tek Prisma® Automated Slide Stainer (Sakura Finetek) according to the manufacturer's instructions. The sections were scanned with a PRECICE500 digital slicing scanning system (Suzhou, China), and scleral thickness was measured by the system's integrated software. Measurements were taken around the optic nerve, and each section was measured three times. The average value was used to indicate the scleral thickness.

Western blot analysis

The eyeball was dissected along the corneal limbus to create an eye cup. Subsequently, the cornea, lens, vitreous body, and retina were removed. The choroid was scraped using fine scissors. The isolated scleral tissue was snap-frozen in liquid nitrogen for further processing.

Table 1. Primer sequences used for qRT-PCR

Gene	Species	Forward (5'-3')	Reverse (5'-3')
Aqp1	Mouse	CGCCACGGCCATTCTC	TTGCGGCCAAGTGAATTG
Hif1α	Mouse	CTGCCACTGCCACCACAACTG	TGCCACTGTATGCTGATGCCTTAG
Mmp9	Mouse	CTGGACAGCCAGACACTAAAG	CTCGCGGCAAGTCTTCAGAG
Col1a1	Mouse	TGACTGGAAGAGCGGAGAGT	GACGGCTGAGTAGGGAACAC
Actb	Mouse	GGAGGAAGAGGATGCGGCA	GAAGCTGTGCTATGTTGCTCTA
Aqp1	Human	GCACACTCTCTTCTCCATTCCC	CATCACAACTCTCCCCACTCCT
Hif-1α	Human	TCCAGCAGACTCAAATACAAGAAC	GTATGTGGGTAGGAGATGGAGATG
Mmp9	Human	GCACCACCACAACATCAC	ACCACAACTCGTCATCGTC
ACTB	Human	GACTTCAACAGCAACTCCCAC	TCCACCACCCTGTTGCTGTA

For western blot analysis, scleral tissues from four eyes in the same group were pooled as one sample for protein extraction. Radioimmunoprecipitation assay (RIPA) lysis buffer (P00-13B; Beyotime, China) supplemented with protease/phosphatase inhibitor cocktail (GRF103; Epizyme, USA) was used for tissue lysis. In addition, minute total protein extraction kit (SD-001, Invent) was utilized for protein extraction. Protein concentrations were determined using the Bradford method, and the same amount of total scleral proteins was separated on 10% sodium dodecyl-sulfate-polyacrylamide gel electrophoresis (SDS-PAGE). Subsequently, the proteins were transferred to polyvinylidene fluoride membranes, followed by incubation with blocking buffer (5% skim milk in 0.1% Tween 20) for 2 h at room temperature. Then, the membranes were subjected to immunoblotting with antibody against Aqp1 (1:1,000, 20333-1-AP, Proteintech Group, China) overnight at 4°C. The following day, the membranes were washed and incubated with horseradish peroxidase (HRP)-conjugated goat anti-rabbit IgG antibody (1:10,000, SA00001-2, Proteintech Group, China) for 1 h at 37°C. The same membrane was stripped and re-probed to detect β-actin (1:20,000, 66009-1-Ig, Proteintech Group, China). The membranes were incubated with HRP substrate (P8S, Beyotime, China), and the protein bands were visualized using a ChemiDoc MP imaging system (Bio-Rad Laboratories, USA). The relative Aqp1 expression level was normalized to β-actin expression level.

Quantitative reverse transcription polymerase chain reaction (qRT-PCR)

The eyeball was dissected along the corneal limbus to create an eye cup. Subsequently, the cornea, lens, vitreous body, and retina were removed. The choroid was scraped using fine scissors. For qRT-PCR, scleral tissues from two eyes in the same group were pooled as one sample for homogenization (TissueLyser II, Qiagen, Germany) and RNA isolation (Trizol reagent, R401, Vazyme, China) according to the manufacturer's instructions. Resulting RNAs were reversely transcribed into complementary DNA (cDNA) using a HiScript IV RT SuperMix for qPCR system (+gDNA wiper) (R423-01, Vazyme) following the manufacturer's protocol. qRT-PCR was performed to determine the transcription levels of *Aqp1*, *Hif1α*, *Mmp9*, *Col1A1* and *Actb*. The gene amplification was conducted in triplicate using a SupRealQ Ultra Hunter SYBR qPCR Master Mix (U+) kit (Q713, Vazyme). The expression level of each target mRNA, relative to that of *Actb*, was determined using threshold cycle values and the $2^{-\Delta\Delta Ct}$ method. The primer sequences are presented in **Table 1**.

For cultured human HSFs, total RNA was isolated using Trizol reagent (R401; Vazyme, China) according to the manufacturer's instructions. cDNA was synthesized from the purified RNA with the HiScript IV RT SuperMix for qPCR system (+gDNA wiper) (R423-01, Vazyme). Expression levels of *Aqp1*, *Hif-1α*, and *Mmp9* genes were quantified using the SupRealQ Ultra Hunter SYBR qPCR Master Mix (U+) kit (Q713, Vazyme). Primer sequences are listed in **Table 1**.

Cell culture and treatments

The human scleral fibroblasts (HSFs) cell line was obtained from the Cell Resource Center, IBMS, CAMS/PUMC (Beijing, China). HSFs were cultured in DMEM High glucose medium (PM150210, Procell, Wuhan) with 10% fetal bovine serum (164210, Procell, China). HSFs

Table 2. Comparison of refraction before and after FDM induction

Time	Diopter (D)			
	DE (n=28)	FE (n=28)	NC-right eye (n=14)	NC-left eye (n=14)
Before	3.88±0.06	3.79±0.08	3.83±0.09	3.84±0.08
After	1.66±0.09	4.92±0.06****	4.78±0.11****	4.91±0.10****

****P<0.0001 vs. FE or NC.

were incubated at 37°C in a normal humidified atmosphere with 5% CO_2.

Construction and transduction of lentivirus

An Aqp1-overexpressing lentiviral vector was commercially generated (OBIO Technology, Shanghai). For transduction, cells were seeded in 6-well plates at 1×10^6 cells/well one day before viral infection. On the day of transduction, the culture medium was replaced with a fresh media containing the lentivirus (1×10^8 TU/mL; MOI=10) and polybrene (5 μg/ml, Sigma-Aldrich, USA). After incubating cells with viral particles-containing media overnight, the medium was replaced with fresh media. After 12 h, Aqp1 overexpression was evaluated by fluorescence microscopy and gene variations were assessed through qRT-PCR.

Construction of a hypoxia model

Totally, 2.5×10^5 HSFs were seeded into 6-well plates for 24 h. When the culture had attained 70-80% confluency, the culture medium was replaced with a serum-free high-glucose DMEM. Hypoxic treatment was performed by placing the cells in a hypoxia chamber (MIC101, Billups-Rothenberg, USA) at 1% O_2 for 12, 24, and 48 hours. The control cells were cultured under normal O_2 conditions (21% O_2) [10]. Cell morphology was studied and photographed at indicated time points using an optical microscope (ZEISS, Germany). The total RNA was subsequently obtained, and the mRNA concentrations of Aqp1 and Hif-1α were analyzed using qRT-PCR.

Impact of acetazolamide treatment under hypoxia

HSFs were exposed to hypoxic conditions and treated with a range of acetazolamide concentrations for 24 h. Subsequently, *Aqp1* expression level was investigated using qRT-PCR to determine an optimal acetazolamide dosing. In the subsequent experiments, HSFs were exposed to acetazolamide at the optimized concentration under hypoxic conditions for 24 and 48 h, and cells were collected for later analyses.

Statistical analysis

All data were analyzed using GraphPad Prism 8.0 software (GraphPad Software Inc., San Diego, CA, USA) and presented as the mean ± standard error (SE). Data normality was examined using the Shapiro-Wilk test, while homogeneity of variances was assessed with the Brown-Forsythe test. For making comparisons between DE and FE eyes from the same animals, a paired t-test was used. For making comparisons involving the NC group (independent samples), the independent-samples t-test was employed. The data from the cell-based experiments were analyzed using the t-test. Comparisons among multiple groups, time points, or concentrations were performed using one-way analysis of variance (ANOVA) followed by Tukey's post hoc test. Statistical analysis was conducted based on data derived from a minimum of three independent experimental replicates. P<0.05 was considered significant, and asterisk symbols were employed to denote degree of statistical significance.

Results

A FDM mouse model generation and validation

It has been well-documented that diopters of mice gradually shift towards hyperopia with increasing age [32]. Therefore, mice diopters in each group were monitored since the beginning of the study. At basal level, the diopters were comparable among all groups with no statistical significance (**Table 2**). However, after 2 weeks of FDM induction, the DE eyes demonstrated a myopic progression (1.66±0.09 D), while the FE and NC eyes exhibited hyperopic progression (FE: 4.92±0.06 D, NC-left eyes: 4.91±0.01 D, NC-right eyes: 4.78±0.11 D) (**Table 2**). Statistical analysis revealed that changes in refraction in experimental groups (in both

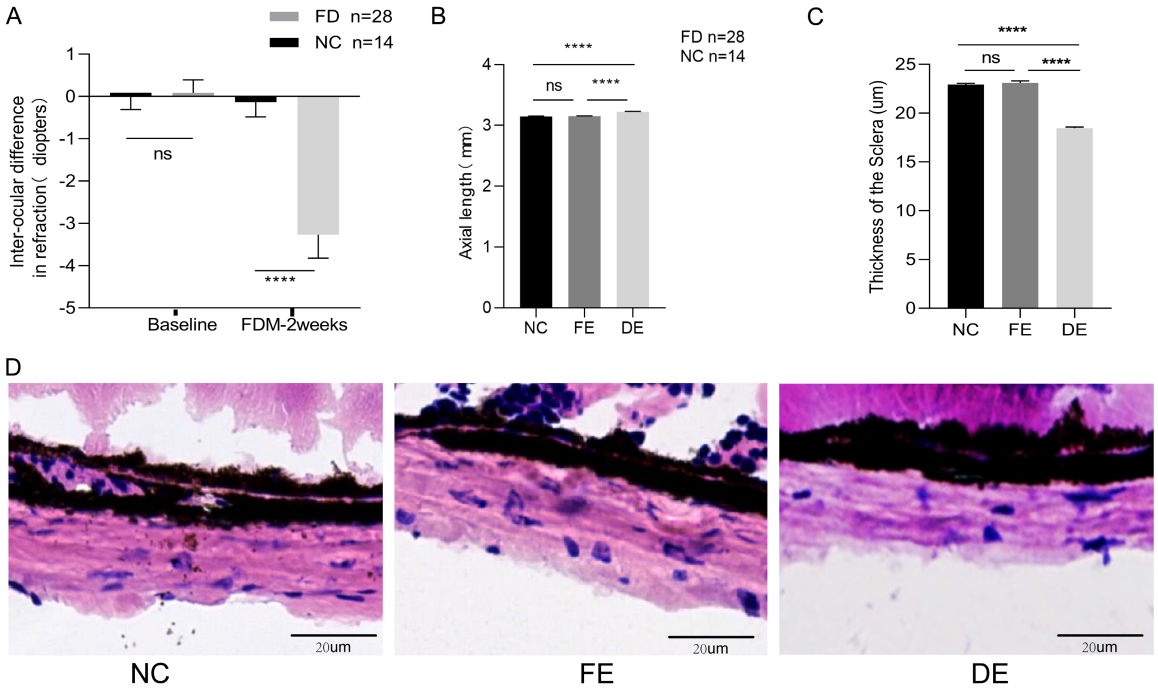

Figure 2. Establishment and validation of the FDM model in mouse. (A) Changes in refraction (diopters) in eyes from the experiment groups and NC groups before and after FDM induction. (B) Comparison of axial length between DE, FE, and NC groups after FDM induction. (C, D) Representative histological staining results (D) and analyzed data (C) of scleral tissues of mice from NC, FE, and DE groups. *P<0.05, ****P<0.0001, vs. NC.

Table 3. Ocular axis length in each group after FDM induction

Time	The axial length (mm)		
	DE (n=28)	FE (n=28)	NC (n=14)
After	3.226±0.005	3.155±0.004****	3.150±0.004****

****P<0.0001 vs. FE or NC.

DE and FE eyes) were significantly different from those in the NC group (**Figure 2A**).

To further validate the ocular changes, axial length of collected eyes in all groups was measured 2 weeks after the FDM induction. The average axial length of the DE eyes was 3.226±0.005 mm, which was significantly elongated compared to the FE group (FE: 3.155±0.004 mm) (**Table 3**). Axial length did not differ significantly between the right and left eyes in the NC group (t=1.228, P=0.2413). Therefore, the axial length in the NC group was calculated from the mean axial length of each NC mouse (3.150±0.004 mm) for comparison with the DE and FE groups (**Figure 2B**). Consequently, significant axial elongation was found in DE eyes compared to FE and NC eyes (P<0.0001). Moreover, histologic analysis was performed to evaluate the morphologic changes in FDM eyes compared to controlled eyes. The results of H&E staining revealed that 2 weeks after myopia induction, the DE eyes exhibited significant thinning of the sclera, as well as reduced cellular density and more loosely collagen arrangement compared with FE and NC groups (**Figure 2C**, **2D**).

Furthermore, Hif-1α expression level was upregulated in mice after myopia induction, and Hif-1α has been identified as a key contributor to myopia development [28, 33]. To validate the success of the FDM modeling, Hif-1α expression level in the sclera was determined using immunofluorescence staining (**Figure 3A**) and qRT-PCR (**Figure 3B**). The results revealed that Hif-1α expression level was significantly upregulated in DE eyes compared with controls (FE and NC eyes), which further validated the success of the FDM modeling.

Investigating Aqp1 expression level in the sclera during myopia development

After successfully establishing the FDM model, the focus shifted to Aqp1 in the sclera. Scleral

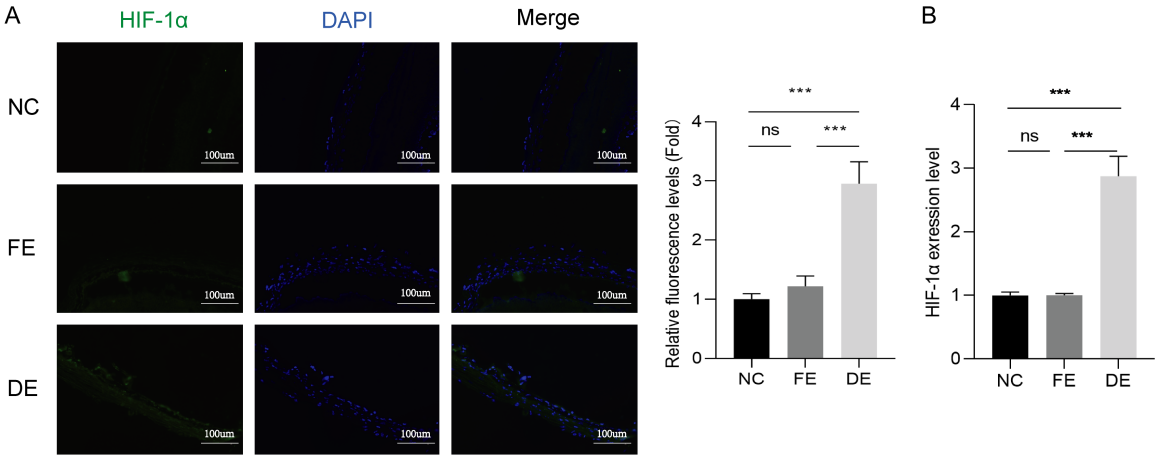

Figure 3. Expression level of Hif-1α in the sclera tissues. A. Representative images of immunofluorescent staining (left panels) and quantified data (right panel) indicating the expression level of Hif-1α in the scleral tissues of mice from indicated groups after myopia modeling. B. Results of qRT-PCR, detecting the mRNA level of Hif-1α in the scleral tissues of mice from indicated groups after myopia modeling. Scale bar =100 μm. *P<0.05, ***P<0.001, vs. NC.

remodeling has been well-documented as a hallmark of myopia development [9]. Previous research has also demonstrated that axial elongation during myopia is associated with scleral remodeling, which is reflected by reduced collagen content and decreased elasticity of the ECM of sclera [9]. As a family of proteins that modulate the aqueous transport and ocular hydration [34], it is reasonable to speculate that AQPs contribute to scleral ECM remodeling. Although Aqp1 has already been observed in the scleral fibroblasts of rats and humans [16], its expression levels and possible contribution to the mouse sclera have not been explored. To address this gap, the expression level of Aqp1 in the mouse sclera was analyzed using the eyeballs of the DE, FE, and NC groups.

Accordingly, the level of Aqp1 expression in the sclera was evaluated using tissues from FDM and NC mice. The results of the immunofluorescent staining showed that Aqp1 was expressed in the sclera of all groups (**Figure 4A**). In addition, it was expressed at a significantly greater level in the DE group than in the FE and NC groups (**Figure 4A**). In the meantime, the qRT-PCR analysis revealed a significantly higher level of Aqp1 mRNA in the sclera of the DE eyes (**Figure 4B**). As is often the case, western blot analysis revealed an upregulation of the Aqp1 protein level in the sclera of the deprived eyes compared to controls (**Figure 4C**). These results showed that the level of Aqp1 expression increased in the sclera as mice developed myopia.

Downregulation of scleral Col1α1 in myopic mice

The sclera is composed of collagen, which accounts for approximately 90% of the scleral dry weight, and type I comprises most of the collagen [35]. This collagen is mainly found in the equatorial and back parts of the eye. Past research has indicated that myopia is associated with structural changes in the scleral collagen, including decreased collagen content and subsequent thinning of the sclera [28, 36].

There was a strong downregulation of scleral expression of Col1α1 in a form-deprived myopia model in mice. Immunofluorescence staining revealed that DE had a lower level of Col1α1 protein than FE and NC (**Figure 5A**). In line with these, the qRT-PCR analysis showed that the mRNA of Col1α1 had been reduced in DE scleral tissues (**Figure 5B**). All of these findings suggested that the downregulation of Col1α1 is a stable characteristic of the myopia progression in mice.

Scleral Mmp9 gene expression increased in myopic mice

MMPs are a family of endopeptidases that are Zn-dependent and are found in many tissues with a strong capacity to degrade collagen. These enzymes are essential in the remodeling

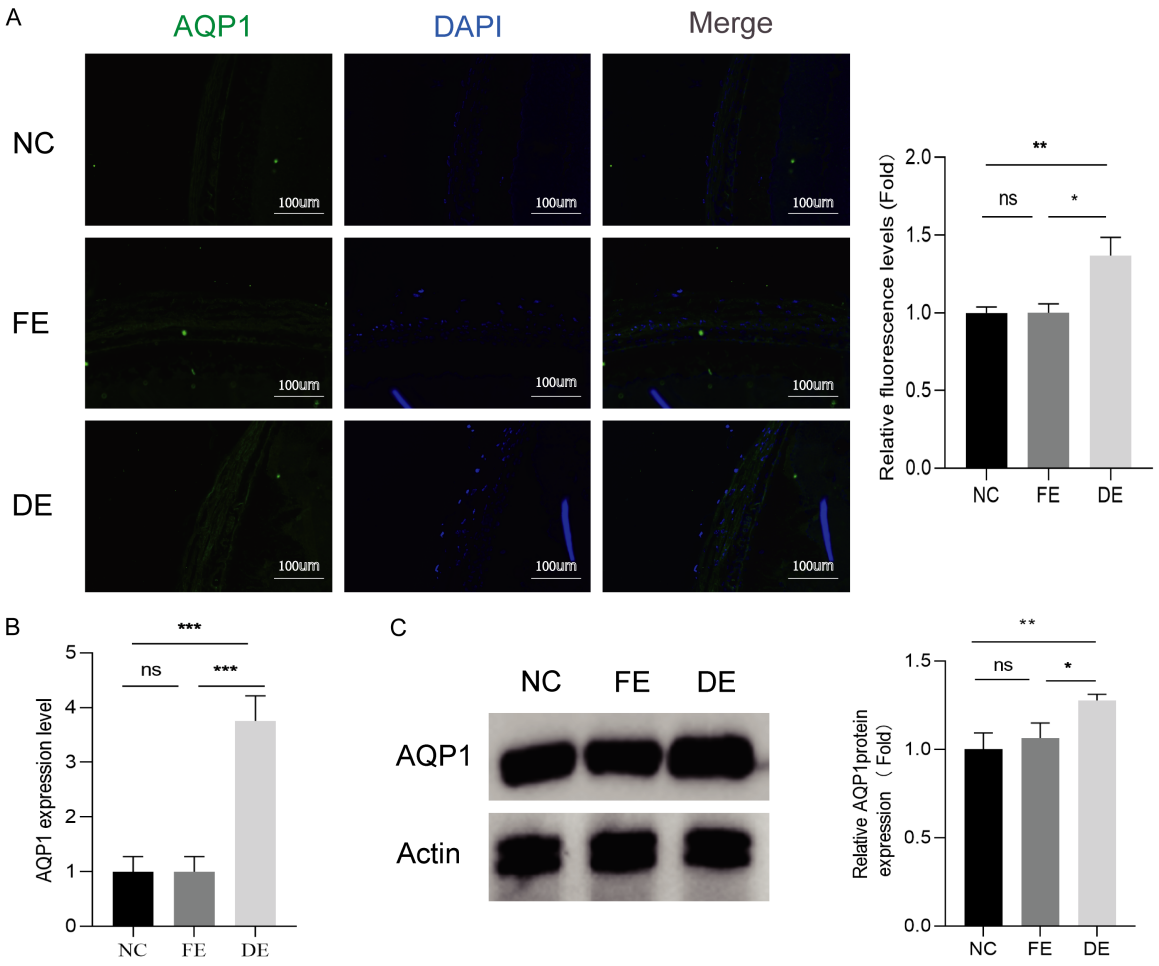

Figure 4. Aqp1 expression in sclera after 2 weeks of FDM induction. A. Representative images of immunofluorescent staining (left panels) and quantified data (right panel) illustrating the expression level of Aqp1 in the scleral tissues of mice from indicated groups after myopia modeling. B. Results of qRT-PCR, detecting the mRNA level of Aqp1 in the scleral tissues of mice from indicated groups after myopia modeling. C. Representative images of western blot analysis (left panel) and quantified results (right panel) demonstrating the expression level of Aqp1 in the scleral tissues of mice from indicated groups after myopia modeling. Scale bar =100 μm. *P<0.05, **P<0.01, ***P<0.001, vs. NC.

of the ECM, especially in specialized locations such as the sclera of the eye [21]. In mouse models of myopia, the expression of MMP-9 increases significantly in the scleral tissue [22]. The immunofluorescence staining revealed low Mmp9 expression level in scleral tissue from all groups, and no significant difference was identified between experimental and control groups (**Figure 6A**). However, results of qRT-PCR showed that Mmp9 mRNA level in DE eyes was significantly higher than that of FE and NC eyes (**Figure 6B**). These findings indicate that Mmp9 may be involved in the early stage of scleral remodeling during myopia development.

Upregulation of Aqp1 expression level in HSFs under hypoxic conditions

Human scleral fibroblasts exhibited a clear, flattened morphology under a microscope, which was characterized by spindle-shaped or stellate-shaped projections. The cells had differentiated, with regularly oval nuclei and huge, conspicuous nucleoli (**Figure 7A**).

Hypoxic conditions were induced using a hypoxia incubator chamber. The morphologic evaluation of HSFs was performed after 12, 24, and 48 hours of exposure to hypoxia (**Figure 7B**). Cells were found to have retained morphology

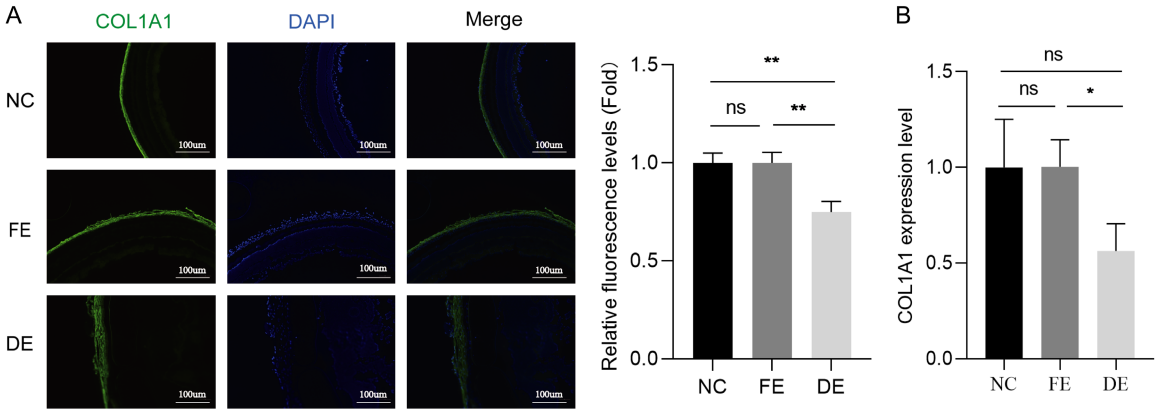

Figure 5. Downregulation of scleral Col1α1 in myopic mice. A. Representative images of immunofluorescent staining (left panels) and quantified data (right panel) indicating the expression level of Col1α1 in the scleral tissues of mice from indicated groups after myopia modeling. B. Results of qRT-PCR showing the mRNA level of Col1a1 in the scleral tissues of mice from indicated groups after myopia modeling. Scale bar =100 μm. **P*<0.05, ***P*<0.01, vs. NC.

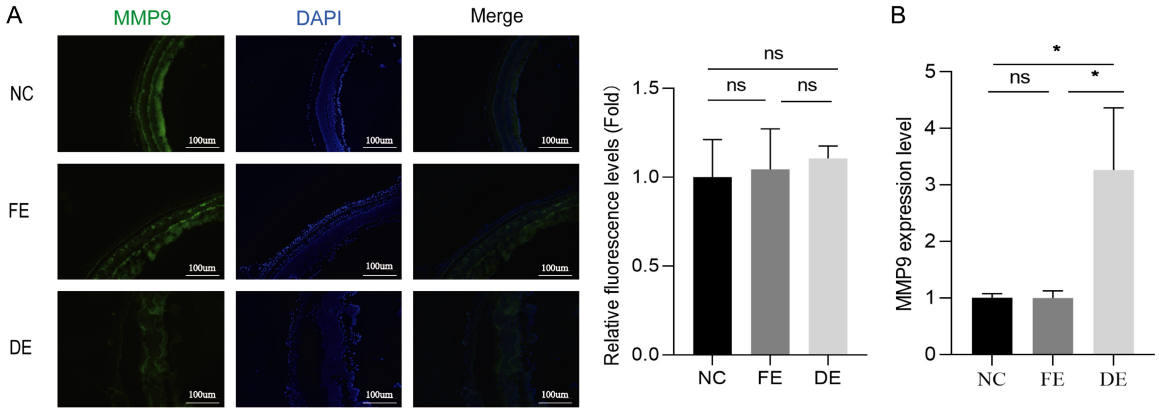

Figure 6. Scleral Mmp9 gene expression increased in myopic mice. A. Representative images of immunofluorescent staining (left panels) and quantified data (right panel), indicating the expression level of Mmp9 in the scleral tissues of mice from indicated groups after myopia modeling. B. Results of qRT-PCR, detecting the mRNA level of Mmp9 in the scleral tissues of mice from indicated groups after myopia modeling. Scale bar =100 μm. **P*<0.05, vs. NC.

after 12, 24, and 48 hours of exposure to hypoxia. As a test of the hypoxic model, qRT-PCR was used to compare the Hif-1α mRNA expression in human scleral fibroblasts (**Figure 7C**). The findings indicated that the level of Hif-1α expression was significantly upregulated in the hypoxia group compared to the control group, confirming the successful establishment of the cellular hypoxia model.

After successful establishment of the cellular hypoxia model, Aqp1 expression level in HSFs was examined. *Aqp1* mRNA level was significantly elevated following 12, 24, and 48 h of hypoxic exposure compared to control cells cultured under normoxic conditions (**Figure 7D**).

Aqp1 modulates Mmp9 expression in human scleral fibroblasts

To explore the controlling effect of Aqp1 on Mmp9 expression, HSFs were stably transduced with lentiviral particles to overexpress Aqp1. Aqp1 overexpression was evaluated by fluorescence microscopy and quantified by qRT-PCR (**Figure 8A**, **8B**). A simultaneous significant increase in Mmp9 mRNA level was noted (**Figure 8C**), indicating that there was a positive regulatory relationship between the Aqp1 and Mmp9 expression in this cellular model.

The level of Aqp1 gene expression did not reach significance after 12 h of hypoxic exposure;

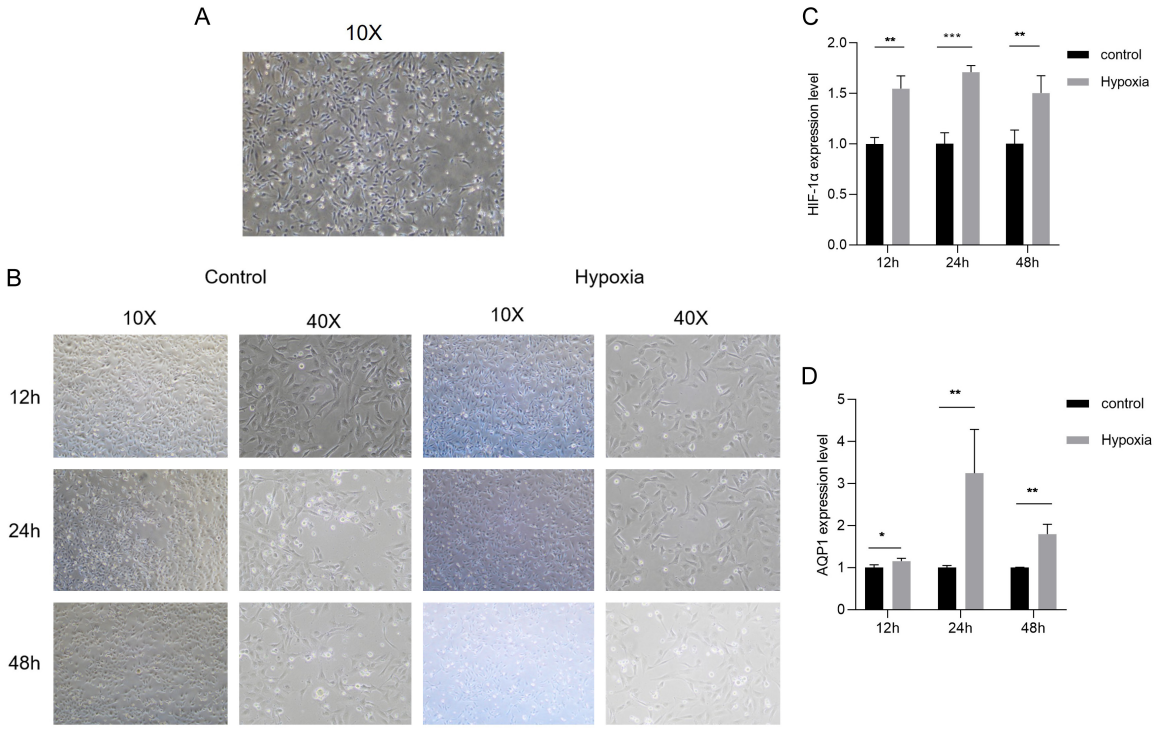

Figure 7. Human scleral fibroblasts (HSFs) exposed to hypoxia conditions. A. The morphology of HSFs under normal conditions (normoxia). B. Morphologic changes of HSFs after 12, 24, and 48 hours of hypoxia exposure. C. Results of qRT-PCR demonstrating the mRNA level of Hif-1α in the HSFs after 12, 24, and 48 hours of hypoxia exposure. D. Results of qRT-PCR detecting the mRNA level of Aqp1 in the HSFs after 12, 24, and 48 hours of hypoxia exposure. *P<0.05, **P<0.01, vs. control.

however, significant differences were identified at 24 and 48 h. Consistently, Mmp9 was significantly upregulated in HSFs after 24 and 48 h of hypoxia (**Figure 8D**). These findings demonstrate that Aqp1 may regulate ECM remodeling via Mmp9.

To verify our speculation, we used acetazolamide, an Aqp1 inhibitor, in a hypoxic environment. An experiment on dose-response (0 to 200 mM acetazolamide and 24 h of hypoxia) was conducted to determine the concentration of acetazolamide that effectively inhibited Aqp1 expression (**Figure 8E**); hence, this concentration was used in subsequent studies.

Under 24 h-hypoxic conditions, acetazolamide inhibition at 200 mM reduced the expression levels of Aqp1 (**Figure 8F**) and Mmp9 (**Figure 8G**). As expected, the expression levels of both Aqp1 (**Figure 8H**) and Mmp9 (**Figure 8I**) were also inhibited by the administration of 200 mM acetazolamide after 48 h of exposure to hypoxia. These findings demonstrate that pharmacologic inhibition of Aqp1 suppresses Mmp9, indicating that the Aqp1-Mmp9 axis is involved in regulating ECM stability under hypoxic conditions.

Discussion

Myopia has become a significant health issue, especially in the East Asian region [1]. It is essential to understand the pathways that lead to myopia development, which will help identify new therapeutic targets. There has been growing evidence that scleral remodeling, characterized by loss of collagen and ECM degradation, is a key factor in myopia pathogenesis [7-9]. Moreover, depletion of Aqp1 has shown to reduce biomechanical strength in the sclera of guinea pigs, demonstrating that Aqp1 contributes to scleral remodeling and the development of myopia [15]. However, the expression level of scleral Aqp1 and its direct relevance to ECM remodeling in myopic mice have not yet been reported. In addition, current *in vitro* studies investigating the effects of Aqp1 on HSFs functionality remain limited and lack systematic evaluation.

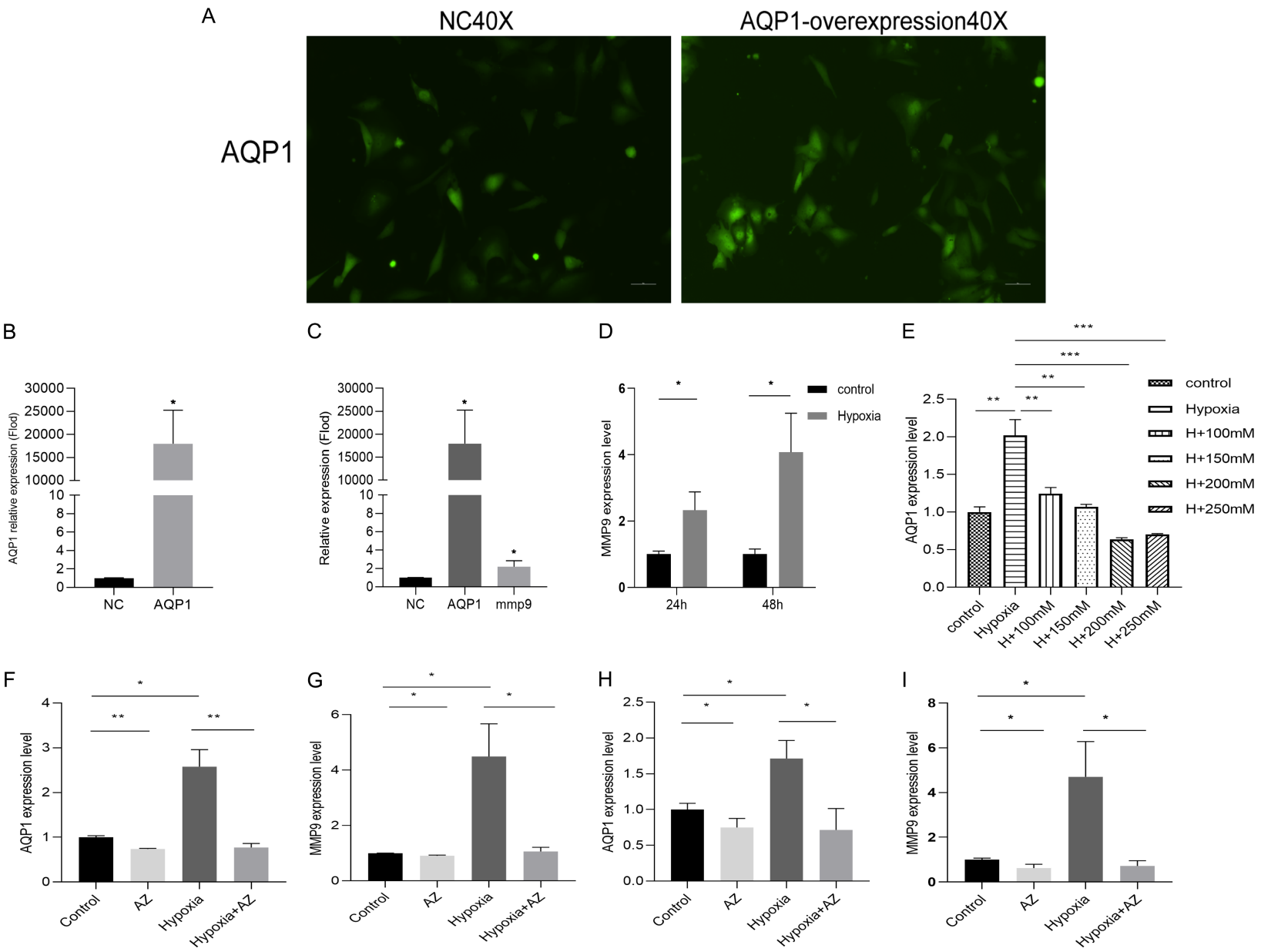
A
NC40X
AQP1-overexpression40X
AQP1
B
AQP1 relative expression (Flod)
NC
AQP1
C
Relative expression (Flod)
NC
AQP1
mmp9
D
MMP9 expression level
control
Hypoxia
24h
48h
E
AQP1 expression level
control
Hypoxia
H+100mM
H+150mM
H+200mM
H+250mM
F
AQP1 expression level
Control
AZ
Hypoxia
Hypoxia+AZ
G
MMP9 expression level
Control
AZ
Hypoxia
Hypoxia+AZ
H
AQP1 expression level
Control
AZ
Hypoxia
Hypoxia+AZ
I
MMP9 expression level
Control
AZ
Hypoxia
Hypoxia+AZ

Figure 8. Aqp1 modulates Mmp9 expression in HSFs. (A) Representative fluorescence microscopy images evaluating Aqp1 overexpression in HSFs. (B) qRT-PCR validation of Aqp1 overexpression. (C) qRT-PCR analysis showing concomitant upregulation of Mmp9 after Aqp1 overexpression. (D) qRT-PCR analysis of Mmp9 mRNA expression in HSFs after 24 and 48 hours of hypoxia. (E) qRT-PCR analysis of Aqp1 mRNA expression under hypoxia (24 h) with indicated concentrations of acetazolamide. (F, G) qRT-PCR analysis of Aqp1 (F), Mmp9 (G) mRNA expression in HSFs after treatment with 200 mM acetazolamide under hypoxia (24 h). (H, I) qRT-PCR analysis of Aqp1 (H) and Mmp9 (I) mRNA expression in HSFs after treatment with 200 mM acetazolamide under hypoxia (48 h). *P<0.05, **P<0.01, vs. control or hypoxia.

Using an established murine model of FDM [37, 38], Aqp1 expression level was found to be upregulated in scleral tissue following myopia induction. Two weeks of form deprivation resulted in significant myopic changes in DE compared with NC and FE, as evidenced by reduced refraction and increased axial length. Additionally, Hif-1α expression level was significantly elevated in the myopic sclera, which was consistent with previous reports [26, 39]. Hypoxia is known to activate signaling pathways in scleral cells that contribute to myopia progression [28]. The concomitant elevation of Hif-1α and Aqp1 in myopic sclera reflects a coordinated transcriptional response, modulating tissue remodeling during myopia development. Hif-1α has been identified as a master regulator of cellular responses to hypoxic stress and has shown to directly stimulate Aqp1 transcription through promoter binding [27]. Moreover, Hif-1α binding to the Aqp1 promoter has been reported, and silencing of Hif-1α reduces Aqp1 expression level under hypoxic conditions [40]. Hif-1α-mediated upregulation of Aqp1 may therefore represent a compensatory mechanism to maintain tissue hydration and structural integrity during axial elongation.

In addition to altered expression levels of Hif-1α and Aqp1, structural changes in the sclera were also evident during myopia development. Alterations in collagen fiber content, diameter, and organization in the sclera during both clinical and experimental myopia have been well documented [4, 38, 39]. Histologic analyses revealed that the sclera of DE eyes was thinner and exhibited more loosely arranged collagen fibers, being consistent with previously reported pathologic features of the myopic sclera. Notably, scleral thinning was accompanied by a significant increase in Aqp1 expression level, indicating a potential functional association between Aqp1 upregulation and scleral remodeling during myopia progression.

The findings demonstrated downregulation of Col1α1, further supporting previous evidence [28]. Earlier studies have reported reduced Col1α1 expression level in the sclera of both clinically diagnosed and experimentally induced myopia [28, 36], a condition characterized by decreased collagen fiber content, reduced fiber diameter, and disorganized collagen architecture. These alterations may be attributed to unbalanced collagen production and degradation, ultimately resulting in scleral thinning (especially in the posterior segment). In pathological myopia, the thickness of posterior sclera could be reduced to 31% of a healthy sclera, significantly compromising its biomechanical strength. As a result, the sclera is weaker and less resistant to physiological intraocular pressure, leading to gradual scleral expansion and notable axial elongation [41]. Given the critical role of collagen for maintaining scleral structure, a possible relationship between Aqp1 and collagen regulation merits investigation. Evidence indicates that Aqp1 is essential for collagen metabolism and is closely associated with type I collagen expression [21, 42, 43]. Furthermore, Aqp1 has shown to influence collagen fiber orientation and crosslinking [44], highlighting its importance in determining tissue biomechanical properties. In addition to regulating scleral hydration and biomechanical strength, Aqp1 may also contribute to scleral remodeling by modulating scleral fibroblast function and ECM synthesis. Future research should investigate whether Aqp1 plays a role in sclera to regulate collagen synthesis, organization, and degradation.

It is well-documented that MMPs play critical roles in collagen metabolism. In the present study, it was found that Mmp9 mRNA level was significantly upregulated after myopia induction, which has been correlated with the expression level of Aqp1 [13]. The absence of detectable Mmp9 upregulation at the protein level in scleral tissues may be attributable to several

factors. First, Mmp9 expression level was assessed at a single time point, during which protein level might be transiently downregulated. Alternatively, post-translational regulatory mechanisms may modulate Mmp9 protein abundance or promote its degradation [45, 46]. In contrast, *in vitro* experiments demonstrated that Aqp1 overexpression in HSFs led to increased Mmp9 mRNA expression and that both genes were co-upregulated under hypoxic conditions. Pharmacologic inhibition of Aqp1 using acetazolamide resulted in concomitant suppression of Mmp9 gene expression. Consistently, previous cancer-based studies have demonstrated that the pro-angiogenic activity of Aqp1 could indirectly influence Mmp9 regulation, indicating a potentially shared mechanism that could also operate in the FDM model [47].

Notably, the upregulation of Mmp9 induced by Aqp1 overexpression was reversed following Aqp1 inhibition with acetazolamide, which was accompanied by a corresponding reduction in Mmp9 expression level. Collectively, these findings indicate that Aqp1 may regulate Mmp9 expression level, thereby influencing ECM stability. It should be acknowledged that acetazolamide is a carbonic anhydrase inhibitor, and its effects on Aqp1 may not be entirely specific. However, human scleral fibroblasts have been reported to exhibit minimal carbonic anhydrase expression [48]. In addition, structural analyses have demonstrated that acetazolamide can interact with loop-E of Aqp1 and inhibit its activity [49]. Furthermore, previous studies have shown that acetazolamide reduces water permeability in cells lacking carbonic anhydrase, supporting a direct effect on Aqp1 function [50]. Taken together, these findings indicate that the observed effects on Mmp9 expression level are most likely attributable to Aqp1 inhibition.

This study revealed that Aqp1 could be upregulated in the sclera of myopic eyes and in human scleral fibroblasts subjected to hypoxia *in vitro*, suggesting that it may be involved in scleral remodeling. The downregulation of Aqp1 in the sclera has, however, shown to cause decreased scleral biomechanical stiffness in guinea pigs [15]. The inconsistency can be explained by the differences in species or a compensatory response to the altered biomechanical strength. These results indicate that Aqp1 plays a more complex role in scleral biomechanics. However, whether it is involved in a feedback loop to modify mechanical forces during axial elongation needs further investigation. Aqp1 upregulation could be a compensatory response to preserve the scleral integrity during axial elongation.

The co-regulated expression changes of Hif-1α, Aqp1, and Mmp9 that occur in the sclera and HSFs in response to hypoxia indicate a possible regulatory relationship among these molecules during myopia development. These findings are consistent with prior investigations, indicating that Hif-1α contributes to myopia development [28, 33]. Moreover, Hif-1α suppression has been linked to the lower level of Aqp1 in the brain and lung [27, 51]. Therefore, it can be speculated that a hypoxic environment in the sclera initiates the transcriptional activity of Hif-1α, which in turn upregulates Aqp1, which promotes scleral remodeling.

Clinically, exploring the connection between Hif-1α and Aqp1 expression levels in myopic eyes may have therapeutic implications. Interventions targeting Hif-1α or Aqp1 can potentially prevent the pathological alterations in the ECM of the sclera when myopia develops. Modulation of scleral biomechanical properties and therapeutic intervention in myopia may be achievable by targeting the Hif-1α/Aqp1 signaling pathway.

Several limitations of this study should be discussed. First, although axial length measurements obtained using digital calipers were informative, accuracy and spatial resolution could be improved in future studies through the use of high-resolution imaging modalities, such as optical coherence tomography. Second, because the present findings were primarily correlative, functional validation through Aqp1 modulation experiments (e.g., gain- or loss-of-function approaches) is required to establish causal relationships. Third, analysis at a single time point provided limited insights into the temporal dynamics of Aqp1 expression level during myopia progression; longitudinal assessments would better characterize these changes. Fourth, the concurrent upregulation of Hif-1α and Aqp1, while indicating a regulatory relationship, was not supported by direct mechanistic evidence, warranting further investigation. Finally, although the FDM model was well established, it might not fully recapitulate the multifactorial etiology of human myopia.

In conclusion, scleral Aqp1 expression level was upregulated during myopia induction. This increase was accompanied by scleral thinning and collagen rearrangement, reflecting a potential association between Aqp1 expression level and scleral remodeling during myopia pathogenesis.

Acknowledgements

We thank Medjaden Inc. for the scientific editing of this manuscript.

Disclosure of conflict of interest

None.

Address correspondence to: Jianlu Gao, Department of Ophthalmology, Liaocheng People's Hospital, Shandong University, Jinan 250012, Shandong, China. E-mail: drgaojianlu@163.com

References

[1] Holden BA, Wilson DA, Jong M, Sankaridurg P, Fricke TR, Smith EL III and Resnikoff S. Myopia: a growing global problem with sight-threatening complications. Community Eye Health 2015; 28: 35.

[2] Pan CW, Cheng CY, Saw SM, Wang JJ and Wong TY. Myopia and age-related cataract: a systematic review and meta-analysis. Am J Ophthalmol 2013; 156: 1021-1033, e1021.

[3] Wu J, Hao J, Du Y, Cao K, Lin C, Sun R, Xie Y and Wang N. The association between myopia and primary open-angle glaucoma: a systematic review and meta-analysis. Ophthalmic Res 2022; 65: 387-397.

[4] Boutin TS, Charteris DG, Chandra A, Campbell S, Hayward C, Campbell A, Nandakumar P, Hinds D, Mitry D and Vitart V. Insights into the genetic basis of retinal detachment. Hum Mol Genet 2020; 29: 689-702.

[5] Chen G, Mao S, Tong Y, Jiang F, Yang J and Li W. Fovea sparing versus complete internal limiting membrane peeling for myopic traction maculopathy: a meta-analysis. Int Ophthalmol 2022; 42: 765-773.

[6] Young TL. Molecular genetics of human myopia: an update. Optom Vis Sci 2009; 86: E8-E22.

[7] Boote C, Sigal IA, Grytz R, Hua Y, Nguyen TD and Girard MJA. Scleral structure and biomechanics. Prog Retin Eye Res 2020; 74: 100773.

[8] Brown DM, Kowalski MA, Paulus QM, Yu J, Kumar P, Kane MA, Patel JM, Ethier CR and Pardue MT. Altered structure and function of murine sclera in form-deprivation myopia. Invest Ophthalmol Vis Sci 2022; 63: 13.

[9] Liu X, Yuan Y, Wu Y, Zhu C, Liu Y and Ke B. Extracellular matrix stiffness modulates myopia scleral remodeling through integrin/F-Actin/YAP axis. Invest Ophthalmol Vis Sci 2025; 66: 22.

[10] Wu W, Su Y, Hu C, Tao H, Jiang Y, Zhu G, Zhu J, Zhai Y, Qu J, Zhou X and Zhao F. Hypoxia-induced scleral HIF-2α upregulation contributes to rises in MMP-2 expression and myopia development in mice. Invest Ophthalmol Vis Sci 2022; 63: 2.

[11] Liu JH, Jin YJ, Wei QQ, Hu YW, Miao XY, Xing YC, Jin YJ and Wang C. Research progress of aquaporins on the ophthalmic diseases. International Eye Science 2022; 22: 420-424.

[12] Li B, Li W, Liu T and Zha L. Extracellular vesicles regulate the transmission of insulin resistance and redefine noncommunicable diseases. Front Mol Biosci 2023; 9: 1024786.

[13] Mu YR, Cai L, Zhou MY, Liu MM, Li Z and Li R. Acetazolamide ameliorates the severity of collagen-induced arthritis in rats: involvement of inducing synovial apoptosis and inhibiting Wnt/β-catenin pathway. Int Immunopharmacol 2021; 90: 107214.

[14] Zhao Y, Zhu H, Yang Y, Ye Y, Yao Y, Huang X, Zhang Y, Shu X, Chen X, Yang Y, Ma J, Cheng L, Wang X and Ying Y. AQP1 suppression by ATF4 triggers trabecular meshwork tissue remodelling in ET-1-induced POAG. J Cell Mol Med 2020; 24: 3469-3480.

[15] Li Z, Chen W, Zhang H and Cui C. The aquaporin-1 depletion downregulates the sclera biomechanical strength. Curr Eye Res 2020; 45: 1240-1244.

[16] Hamann S, Zeuthen T, La Cour M, Nagelhus EA, Ottersen OP, Agre P and Nielsen S. Aquaporins in complex tissues: distribution of aquaporins 1-5 in human and rat eye. Am J Physiol 1998; 274: C1332-1345.

[17] Yamashita T, Asano Y, Saigusa R, Taniguchi T, Nakamura K, Miura S, Toyama T, Takahashi T, Ichimura Y, Hirabayashi M, Yoshizaki A, Miyagaki T, Sugaya M and Sato S. Increased expression of aquaporin-1 in dermal fibroblasts and dermal microvascular endothelial cells possibly contributes to skin fibrosis and edema in patients with systemic sclerosis. J Dermatol Sci 2019; 93: 24-32.

[18] Montiel V, Bella R, Michel LYM, Esfahani H, De Mulder D, Robinson EL, Deglasse JP, Tiburcy M, Chow PH, Jonas JC, Gilon P, Steinhorn B, Michel T, Beauloye C, Bertrand L, Farah C, Dei Zotti F, Debaix H, Bouzin C, Brusa D, Horman S, Vanoverschelde JL, Bergmann O, Gilis D, Rooman M, Ghigo A, Geninatti-Crich S, Yool A, Zimmermann WH, Roderick HL, Devuyst O and

Balligand JL. Inhibition of aquaporin-1 prevents myocardial remodeling by blocking the transmembrane transport of hydrogen peroxide. Sci Transl Med 2020; 12: eaay2176.
[19] Zhan X, Zhu ZC, Sun SQ and Wen YC. Dynamic changes of activator protein 1 and collagen I expression in the sclera of myopia guinea pigs. Int J Ophthalmol 2019; 12: 1272-1276.
[20] Hua Y, Ying X, Qian Y, Liu H, Lan Y, Xie A and Zhu X. Physiological and pathological impact of AQP1 knockout in mice. Biosci Rep 2019; 39: BSR20182303.
[21] Rim YA, Nam Y, Park N, Lee K, Jung H, Jung SM, Lee J and Ju JH. Characterization of early-onset finger osteoarthritis-like condition using patient-derived induced pluripotent stem cells. Cells 2021; 10: 317.
[22] Chen J, Ikeda SI, Yang Y, Zhang Y, Ma Z, Liang Y, Negishi K, Tsubota K and Kurihara T. Scleral remodeling during myopia development in mice eyes: a potential role of thrombospondin-1. Mol Med 2024; 30: 25.
[23] Wei X and Dong J. Aquaporin 1 promotes the proliferation and migration of lung cancer cell in vitro. Oncol Rep 2015; 34: 1440-1448.
[24] Yu Q and Zhou JB. Scleral remodeling in myopia development. Int J Ophthalmol 2022; 15: 510-514.
[25] Jo MS, Yang HW, Park JH, Shin JM and Park IH. Glycolytic reprogramming is involved in tissue remodeling on chronic rhinosinusitis. PLoS One 2023; 18: e0281640.
[26] Zhao F, Zhang D, Zhou Q, Zhao F, He M, Yang Z, Su Y, Zhai Y, Yan J, Zhang G, Xue A, Tang J, Han X, Shi Y, Zhu Y, Liu T, Zhuang W, Huang L, Hong Y, Wu D, Li Y, Lu Q, Chen W, Jiao S, Wang Q, Srinivasalu N, Wen Y, Zeng C, Qu J and Zhou X. Scleral HIF-1alpha is a prominent regulatory candidate for genetic and environmental interactions in human myopia pathogenesis. EBioMedicine 2020; 57: 102878.
[27] Abreu-Rodríguez I, Sánchez Silva R, Martins AP, Soveral G, Toledo-Aral JJ, López-Barneo J and Echevarría M. Functional and transcriptional induction of aquaporin-1 gene by hypoxia; analysis of promoter and role of Hif-1α. PLoS One 2011; 6: e28385.
[28] Wu H, Chen W, Zhao F, Zhou Q, Reinach PS, Deng L, Ma L, Luo S, Srinivasalu N, Pan M, Hu Y, Pei X, Sun J, Ren R, Xiong Y, Zhou Z, Zhang S, Tian G, Fang J, Zhang L, Lang J, Wu D, Zeng C, Qu J and Zhou X. Scleral hypoxia is a target for myopia control. Proc Natl Acad Sci U S A 2018; 115: E7091-E7100.
[29] Lu Y, Song W, Li Y, Xiao J, Du K, Fu Q, Zhang Y, Zhao L, Yin Y, Hu T and Wen D. Mechanisms of no-mediated protein S-nitrosylation in the lens-induced myopia. Oxid Med Cell Longev 2022; 2022: 8296043.
[30] Wu Y, Luo X, Feng Y, Yang J, Fan H, Cen X and Li W. Comparison of the accuracy of axial length measurement by different imaging methods in Sprague Dawley rats. Front Neurosci 2023; 16: 1106904.
[31] Orchard GE, Shams M, d'Amico C, Wojcik K, Ismail F, Mohammad M, Salih R, Shams F and Mallipeddi R. New embedding and staining systems PrestoCHILL and Presto stainer for application in the advancement of Mohs micrographic surgery. Br J Biomed Sci 2017; 74: 203-208.
[32] Liu SS, Shi MH and Zhang HM. Influencing factors and research progress in the mouse model of myopia. Chin J Exp Ophthalmol 2024; 42: 1065-1072.
[33] Yin Y, Zhang X, Han Y, Song J and Bi H. mTOR/HIF-1α-associated scleral metabolic reprogramming by Mingshi formula in form-deprivation myopia. Sci Rep 2025; 15: 37204.
[34] Goel M, Picciani RG, Lee RK and Bhattacharya SK. Aqueous humor dynamics: a review. Open Ophthalmol J 2010; 4: 52-59.
[35] Jan C, Li L, Keay L, Stafford RS, Congdon N and Morgan I. Prevention of myopia, China. Bull World Health Organ 2020; 98: 435-437.
[36] Desmettre T, Gatinel D and Leveziel N. Epigenetics and myopia: mechanisms and therapeutic targets. J Fr Ophtalmol 2022; 45: 1209-1216.
[37] Ma Y and You Y. Animal models and induction methods of myopia. Int Rev Ophthalmol 2023; 47: 503-507.
[38] Chen Y. Study on the role and mechanism of scleral deubiquitinating enzyme Usp7 in mouse form-deprivation myopia. Wenzhou Medical University 2021.
[39] Lin SS, Wu JF and Jiang WJ. Research progress on the mechanism of hypoxia-inducible factor 1α in the development and progression of ophthalmic diseases. Shandong Medical Journal 2023; 63: 105-107.
[40] Zhang J, Xiong Y, Lu LX, Wang H, Zhang YF, Fang F, Song YL and Jiang H. AQP1 expression alterations affect morphology and water transport in Schwann cells and hypoxia-induced up-regulation of AQP1 occurs in a HIF-1α-dependent manner. Neuroscience 2013; 252: 68-79.
[41] McMonnies CW. An examination of the baropathic nature of axial myopia. Clin Exp Optom 2014; 97: 116-124.
[42] Patil R, Wang H, Sharif NA and Mitra A. Aquaporins: novel targets for age-related ocular disorders. J Ocul Pharmacol Ther 2018; 34: 177-187.
[43] Huo Q, Wang T, Wang T and Zhang R. Acetazolamide attenuates cardiac fibrosis induced by aortic constriction through inhibiting transforming growth factor-β1/Smad2 signaling pathway in mice. Exp Ther Med 2019; 17: 2317-2321.

[44] Agbani EO, Williams CM, Li Y, van den Bosch MT, Moore SF, Mauroux A, Hodgson L, Verkman AS, Hers I and Poole AW. Aquaporin-1 regulates platelet procoagulant membrane dynamics and in vivo thrombosis. JCI Insight 2018; 3: e99062.
[45] Surgucheva I, Chidambaram K, Willoughby DA and Surguchov A. Matrix metalloproteinase 9 expression: new regulatory elements. J Ocul Biol Dis Infor 2010; 3: 41-52.
[46] Włodarczyk L, Cichon N, Karbownik MS, Saluk J and Miller E. Exploring the role of MMP-9 and MMP-9/TIMP-1 ratio in subacute stroke recovery: a prospective observational study. Int J Mol Sci 2024; 25: 5745.
[47] Tomita Y, Dorward H, Yool AJ, Smith E, Townsend AR, Price TJ and Hardingham JE. Role of aquaporin 1 signalling in cancer development and progression. Int J Mol Sci 2017; 18: 299.
[48] Hageman GS, Zhu XL, Waheed A and Sly WS. Localization of carbonic anhydrase IV in a specific capillary bed of the human eye. Proc Natl Acad Sci U S A 1991; 88: 2716-2720.
[49] Gao J, Wang X, Chang Y, Zhang J, Song Q, Yu H and Li X. Acetazolamide inhibits osmotic water permeability by interaction with aquaporin-1. Anal Biochem 2006; 350: 165-170.
[50] Ma B, Xiang Y, Mu SM, Li T, Yu HM and Li XJ. Effects of acetazolamide and anordiol on osmotic water permeability in AQP1-cRNA injected Xenopus oocyte. Acta Pharmacol Sin 2004; 25: 90-97.
[51] Keskinidou C, Lotsios NS, Vassiliou AG, Dimopoulou I, Kotanidou A and Orfanos SE. The interplay between aquaporin-1 and the hypoxia-inducible factor 1α in a lipopolysaccharide-induced lung injury model in human pulmonary microvascular endothelial cells. Int J Mol Sci 2022; 23: 10588.